

Effects of nonzero photon momentum in $(\gamma, 2e)$ processes*

A G Galstyan^{1†}, O Chuluunbaatar², Yu V Popov^{3‡} and B Piraux⁴

¹ *Physics Faculty, Moscow State University, Moscow, Russia*

² *Joint Institute for Nuclear Research, Dubna, Russia*

³ *Skobeltsyn Institute of Nuclear Physics, Moscow State University, Moscow, Russia*

⁴ *Institute of Condensed Matter and Nanosciences, Université catholique de Louvain, 2, chemin du cyclotron, BOX L7.01.07, B1348 Louvain-la Neuve, Belgium*

We study the effects of nonzero photon momentum on the triply-differential cross section for $(\gamma, 2e)$ processes. Due to the low value of the photon momentum, these effects are weak and manifest only in special kinematical conditions like the back-to-back emission of the electrons with equal energy sharing. Helium and a few light helium-like ions are treated in detail. Quite unexpectedly, the magnitude of these effects is maximal for relatively small photon energies. However, although this effect on the TDCS remains rather small, of the order of a few mbarn $eV^{-1} sr^{-2}$, it is sufficient to be observed experimentally.

PACS numbers: 32.80.Fb, 31.30.jn

I. INTRODUCTION

At present, most of the theoretical studies of the interaction of atoms and molecules with external electric (laser) fields assume that the vector potential \vec{A} depends only on time. This, of course, results from the dipole approximation. This approximation is usually extremely good. However, in general, $\vec{A}(\vec{r}, t)$ depends also on \vec{r} . In the present contribution, we take into account this dependence by decomposing $\vec{A}(\vec{r}, t)$ in a basis of plane waves $\exp(\pm i(\omega t - \vec{k} \cdot \vec{r}))$ where ω is the photon frequency and \vec{k} its momentum. Note that even for one photon transitions, the vector potential (electric field) depends always on the space coordinate. However, since $k = \omega/c$, the actual value of k is usually very small so that its effects are expected to manifest only at rather high frequencies.

To our knowledge, Amusia *et al.* were the first to consider theoretically one-photon double ionization of helium at non relativistic electron energies while taking into account the nonzero photon momentum in their perturbative calculations [1]. They found one more process, the so-called "sea-gull" diagram, which contributes to the amplitude. This process does occur only if $k \neq 0$. In addition, their calculations suggest that the amplitude of the effects is sensitive to the way the helium initial and final state wave functions behave in the cusp region where the interelectron distance tends to zero. Unfortunately, at the time their paper was published, the authors could only treat the electron-electron interaction in the final state as a perturbation. Recently, Ludlow *et al.* [2] using their time-dependent close coupling method, found a peak in the quadrupole energy distribution of the escaping electrons at 800 eV photon energy. This peak that corresponds to equal energy sharing is a signature of the above process and disappears completely when the photon momentum is zero. Later on, evidence of this effect has been found experimentally [3].

In this contribution, we use the time independent perturbation theory to analyze Amusia's process in the case of linearly and elliptically polarized fields. Contrary to Ludlow *et al.*, all multipole interactions are taken into account. In addition, our helium initial and final state wave functions satisfy the Kato cusp condition. We calculate the triply-differential cross section (TDCS) and try to evaluate accurately the relative importance of the multipole transitions when compared to the dipole ones.

Atomic units $\hbar = e = m_e = 1$ are used throughout unless otherwise specified.

* Submitted to PRA: RAPID COMMUNICATIONS

† galstyan@physics.msu.ru

‡ popov@srd.sinp.msu.ru

II. THEORY

A. Linear polarization

We have to calculate the following matrix element [4]

$$M(\vec{k}) = \int \Psi_f^{-*}(\vec{r}_1, \vec{r}_2) \left[e^{i\vec{k}\cdot\vec{r}_1} (\vec{\epsilon} \cdot \hat{p}_1) + e^{i\vec{k}\cdot\vec{r}_2} (\vec{\epsilon} \cdot \hat{p}_2) \right] \Psi_i(\vec{r}_1, \vec{r}_2) d^3r_1 d^3r_2. \quad (1)$$

Here $\hat{p}_j \equiv -i\vec{\nabla}_j$, $j = 1, 2$. The functions Ψ are wave functions solution of the field free helium Hamiltonian. For clarity, we define the coordinates of all vectors as follows: $\vec{\epsilon} = \{0, 0, 1\}$ is the unit vector along the polarization axis that coincides with the z -axis; the outgoing electron momenta are $\vec{p}_1 = p_1 \{\sin \theta_1 \cos \varphi_1, \sin \theta_1 \sin \varphi_1, \cos \theta_1\}$ and $\vec{p}_2 = p_2 \{\sin \theta_2 \cos \varphi_2, \sin \theta_2 \sin \varphi_2, \cos \theta_2\}$ and the photon momentum $\vec{k} = \omega/c \{\cos \phi; \sin \phi; 0\}$. The energy conservation writes $\omega + \varepsilon_0^{He} = p_1^2/2 + p_2^2/2$ where ε_0^{He} is the helium ground state energy. The TDCS is given by ($\alpha = c^{-1} = 1/137$):

$$\frac{d^3\sigma}{d\Omega_1 d\Omega_2 dE_1} = 2 \frac{\alpha p_1 p_2}{(2\pi)^4 \omega} \left[\frac{1}{2\pi} \int_0^{2\pi} |M(\vec{k})|^2 d\phi \right]. \quad (2)$$

In most of the experimental geometries and kinematical conditions, k is rather small compared to the electron momenta. As a result, it is straightforward to show that in very good approximation,

$$M(\vec{k}) = M(0) + \left[(\vec{k} \cdot \vec{p}_1) g_1 + (\vec{k} \cdot \vec{p}_2) g_2 \right] + O(k^2). \quad (3)$$

Eq. (3) shows that an effect of the nonzero photon momentum can be seen in the angular domain where $M(0) \sim 0$. It is well known [5] that, for equal energy sharing, *i.e.* when $p_1 = p_2$, the matrix element $M(0) = 0$ if $\vec{p}_1 = -\vec{p}_2$ (back-to-back emission, $\theta_2 = \pi - \theta_1$, $\varphi_2 = \pi + \varphi_1$). Let us consider the coplanar case, when both momenta are disposed in the plane (x, z): $\vec{p}_1 = p_1 \{\sin \theta, 0, \cos \theta\}$ and $\vec{p}_2 = p_1 \{-\sin \theta, 0, -\cos \theta\}$. In this geometry, it is now possible to separate the ϕ and θ dependence and write:

$$M(\vec{k}) \approx k \cos \phi G(\theta), \quad (4)$$

where the expression of $G(\theta)$ is, for the time being, unspecified. Averaging on the variable ϕ in (2) is trivial: $\overline{|M(\vec{k})|^2} = 1/2 |M(\vec{k})_{\phi=0}|^2$. In the general case, $\overline{|M(\vec{k})|^2} \approx |M(0)|^2 + 1/2 |M(\vec{k})_{\phi=0} - M(0)|^2$.

In order to estimate the magnitude of the TDCS, we use the same initial and final wave functions considered in the model described earlier in [6]. The properly normalized and correlated initial state wave function is given by:

$$\Psi_i(\vec{r}_1, \vec{r}_2) = \sum_j D_j (e^{-a_j r_1 - b_j r_2} + e^{-a_j r_2 - b_j r_1}) e^{-\gamma_j r_{12}}, \quad (5)$$

giving the helium ground energy $\varepsilon_0^{He} = -2.90372$ a.u.. The final double continuum wave function is given by the well known 3C function:

$$\Psi_f^{(-)}(\vec{r}_1, \vec{r}_2) = e^{i\vec{p}_{12} \cdot \vec{r}_{12}} \phi_1^{-*} \phi_2^{-*} \phi_{12}^{-*}. \quad (6)$$

Here

$$\phi_j^{-*}(\vec{p}_j, \vec{r}) = R(\xi_j) e^{-i\vec{p}_j \cdot \vec{r}} {}_1F_1[-i\xi_j, 1; i(p_j r + \vec{p}_j \cdot \vec{r})],$$

with

$$\vec{p}_{12} = \frac{1}{2}(\vec{p}_1 - \vec{p}_2); \quad \xi_{12} = \frac{1}{2p_{12}}; \quad \xi_j = -\frac{2}{p_j} \quad (j = 1, 2); \quad R(\xi) = e^{-\pi\xi/2} \Gamma(1 + i\xi).$$

In these conditions, we are left with the evaluation of the following 3-dimensional integral:

$$M(\vec{k}) = i \sum_j D_j \int \frac{d^3p}{(2\pi)^3} \{ \gamma_j K_{12}(\vec{p}_{12}; \vec{p}_{12} - \vec{p}; \vec{\epsilon}; \gamma_j) \times \left[\frac{\partial I_1(\vec{p}_1; \vec{k} + \vec{p}; a_j)}{\partial a_j} \frac{\partial I_2(\vec{p}_2; -\vec{p}; b_j)}{\partial b_j} - \frac{\partial I_2(\vec{p}_2; \vec{k} - \vec{p}; a_j)}{\partial a_j} \frac{\partial I_1(\vec{p}_1; \vec{p}; b_j)}{\partial b_j} + (a_j \rightleftharpoons b_j) \right] + \frac{\partial I_{12}(\vec{p}_{12}; \vec{p}_{12} - \vec{p}; \gamma_j)}{\partial \gamma_j} \times \left[a_j K_1(\vec{p}_1; \vec{k} + \vec{p}; \vec{\epsilon}; a_j) \frac{\partial I_2(\vec{p}_2; -\vec{p}; b_j)}{\partial b_j} + a_j K_2(\vec{p}_2; \vec{k} - \vec{p}; \vec{\epsilon}; a_j) \frac{\partial I_1(\vec{p}_1; \vec{p}; b_j)}{\partial b_j} + (a_j \rightleftharpoons b_j) \right] \}. \quad (7)$$

In (7),

$$I_x(\vec{p}_x, \vec{p}, \lambda) = \int \frac{d^3r}{r} e^{i\vec{p}\cdot\vec{r}} \phi_x^{-*}(\vec{p}_x, \vec{r}) e^{-\lambda r} = 4\pi R(\xi_x) \frac{[(\lambda - ip_x)^2 + p^2]^{i\xi_x}}{[(\vec{p} - \vec{p}_x)^2 + \lambda^2]^{(1+i\xi_x)}}, \quad (8)$$

and

$$\begin{aligned} K_x(\vec{p}_x, \vec{p}, \vec{e}, \lambda) &= \int \frac{d^3r}{r} e^{i\vec{p}\cdot\vec{r}} \phi_x^{-*}(\vec{p}_x, \vec{r}) (\vec{e} \cdot \vec{r}) e^{-\lambda r} \\ &= -2iI_x(\vec{p}_x, \vec{p}, \lambda) \left[i\xi_x \frac{\vec{e} \cdot \vec{p}}{(\lambda - ip_x)^2 + p^2} - (1 + i\xi_x) \frac{\vec{e} \cdot (\vec{p} - \vec{p}_x)}{(\vec{p} - \vec{p}_x)^2 + \lambda^2} \right]. \end{aligned} \quad (9)$$

The first term in the figure brackets in the rhs of Eq. 7 just corresponds to the "sea-gull" graph discussed in [1] and disappears if $k = 0$.

B. Elliptic polarization

In the case of elliptically polarized photons, we have $\vec{e} = \{i \sin \beta, 0, \cos \beta\}$ with $-\pi/2 \leq \beta \leq \pi/2$, and $\vec{k} = \alpha\omega\{0, 1, 0\}$. The case $\beta = 0$ corresponds to the linear polarization.

III. RESULTS AND DISCUSSION

In Fig.1, we consider the case $k = 0$ and compare our results for the absolute TDCS as a function of θ_2 with the data of two experiments, by Schwartzkopf and Schmidt [7] and Brauning *et al.* [8]. In both cases, the photon energy is equal to 99 eV, the two electrons share the same energy, $E_1 = E_2 = 10$ eV and \vec{p}_1 is along the polarization axis. The qualitative agreement of our results with the experimental data of Brauning *et al.* and the fact that it is also

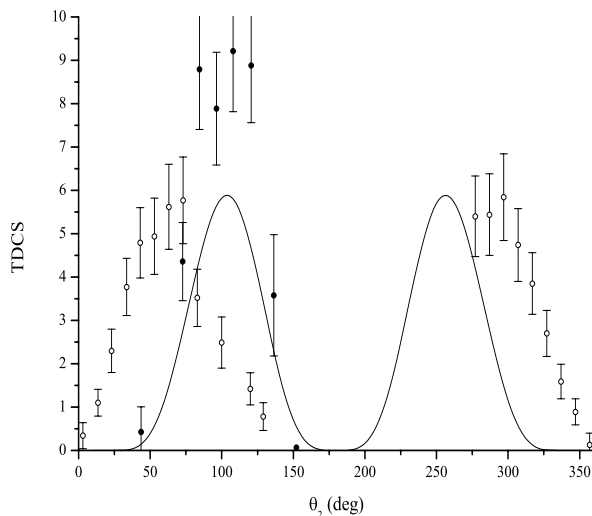


FIG. 1: Absolute TDCS in $\text{b eV}^{-1} \text{sr}^{-2}$ (given by (2)) as a function of θ_2 , the angle between \vec{p}_2 and the polarization axis. The photon momentum $k = 0$, $\omega = 99$ eV, \vec{p}_1 is directed along the polarization axis and $E_1 = E_2 = 10$ eV. Our results (full line) are compared to the data of two experiments: open circles, Schwartzkopf and Schmidt [7] and black dots, Brauning *et al.* [8].

the case with other theoretical approaches that reproduce the correct peak position seem to suggest that there is a problem with the experimental results of Schwartzkopf and Schmidt. On the other hand, it is legitimate to expect that the present model gives at least reliable qualitative results. In Fig.2, we consider the case of a back-to-back electron emission ($\vec{p}_1 = -\vec{p}_2$). The averaged TDCS is shown as a function of the angles θ and φ of the escaping

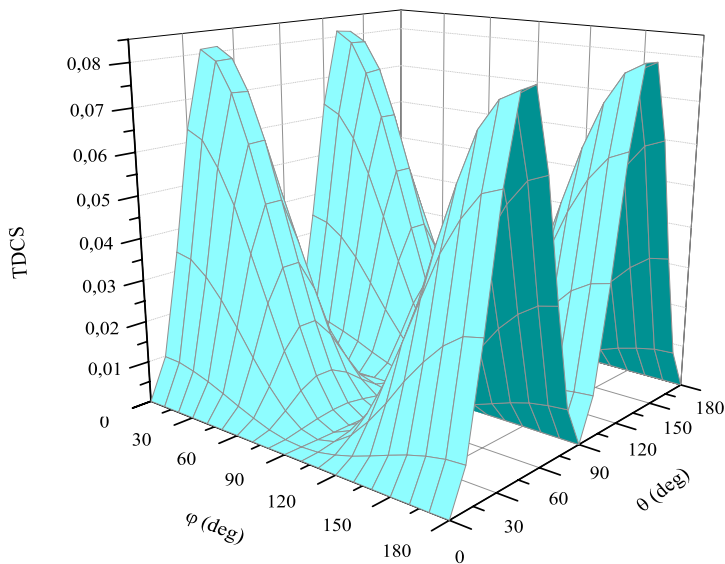


FIG. 2: (Color online) Absolute averaged TDCS in $\text{mb eV}^{-1} \text{sr}^{-2}$ in the case of a back-to-back electron emission. $\vec{p}_1 = -\vec{p}_2 = p\{\sin\theta \cos\varphi, \sin\theta \sin\varphi, \cos\theta\}$, $\omega = 799 \text{ eV}$, $E_1 = E_2 = 360 \text{ eV}$ and $k = \alpha\omega$.

electrons. The kinetic energy of each electron is $E = 360 \text{ eV}$. Note that for a back-to-back emission, the electron energy distribution presents a local maximum at equal energy sharing [2] (see also Fig. 6 taking into account that $M(0) = 0$). We clearly see a 4-peak angle distribution. This contrasts with the zero photon momentum case where this distribution is uniformly zero. Of course, the effect is very small, the magnitude of it being of the order of a fraction of millibarn. This effect is also observable in Fig. 3 for the same case as in Fig. 2. Here, however, the angle

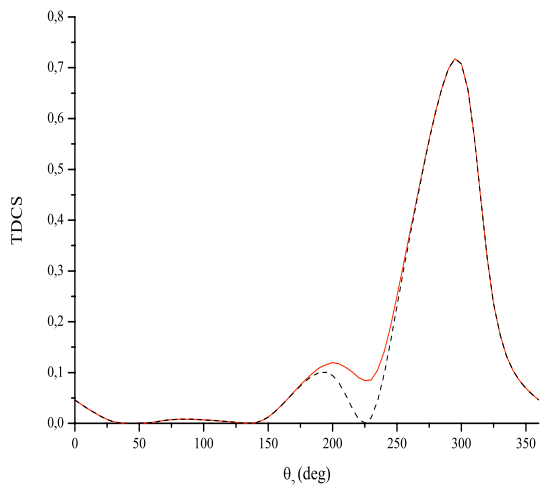


FIG. 3: (Color online) Absolute TDCS in $\text{mb eV}^{-1} \text{sr}^{-2}$ (given by (2) and therefore averaged over the variable ϕ) as a function of θ_2 for $\omega = 799 \text{ eV}$ and $E_1 = E_2 = 360 \text{ eV}$. It is assumed that the angle θ_1 between the momentum \vec{p}_1 and the polarization axis is fixed to 45° . In addition, the direction of the vector \vec{p}_2 rotates with θ_2 in the plane formed by \vec{p}_1 and the polarization axis. Two different values of the photon momentum k are considered: $k = 0$ (dotted line) and $k = \alpha\omega$ (full line).

between the electron momentum \vec{p}_1 and the polarization vector is fixed at 45° . These two vectors form a plane in which \vec{p}_2 rotates. The TDCS is shown as a function of θ_2 for two values, namely 0 and $\alpha\omega$ of the photon momentum

k . The peak at $\theta_2 = 215^\circ$ for $k = \alpha\omega$ is about twice higher than the value obtained for $k = 0$ but again, the effect is rather small.

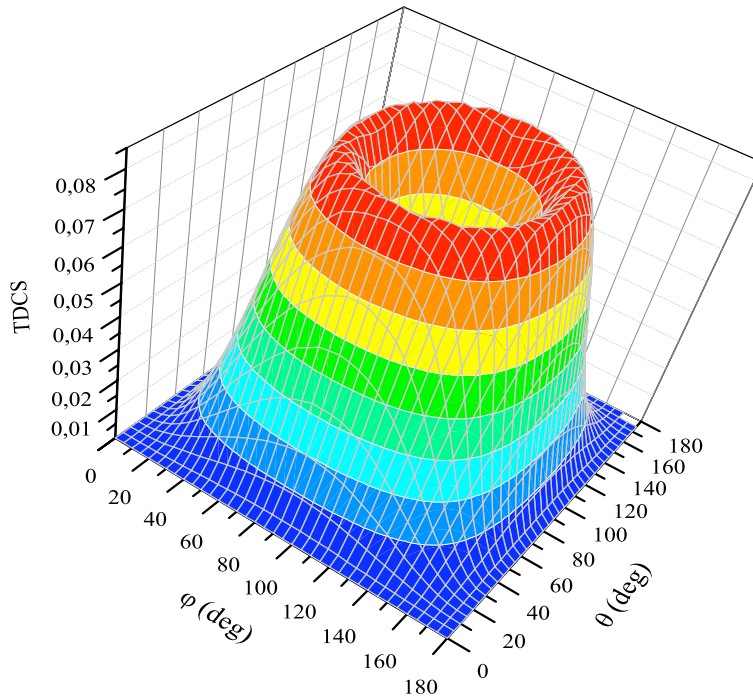


FIG. 4: (Color online) Absolute TDCS in $\text{mb eV}^{-1} \text{sr}^{-2}$ in the case of a back-to-back electron emission. Angles θ and φ are the same like in Fig. 2, $\omega = 799 \text{ eV}$, $E_1 = E_2 = 360 \text{ eV}$ and $k = \alpha\omega$. In this case, the field is circularly polarized, $\beta = 45^\circ$.

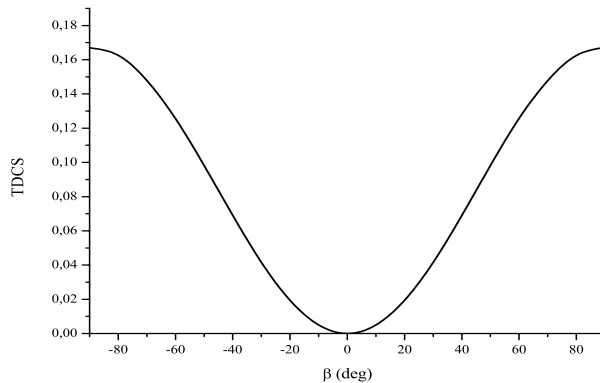


FIG. 5: Absolute TDCS in $\text{mb eV}^{-1} \text{sr}^{-2}$ for $\theta = 90^\circ$, $\varphi = 135^\circ$ as a function of β that determines the polarization of the field. As in Fig. 2, the photon energy is equal to 799 eV, $k = \alpha\omega$ and it is assumed that both electrons are emitted back-to-back with $E_1 = E_2 = 360 \text{ eV}$.

So far, we have considered the case of a linear polarization. Let us now assume the field circularly polarized. In Fig. 4, we consider the same case as in Fig. 2 except that β which determines the type of field polarization is now equal to 45° , what corresponds to the circular polarization. The TDCS as a function of θ and φ exhibits a volcano

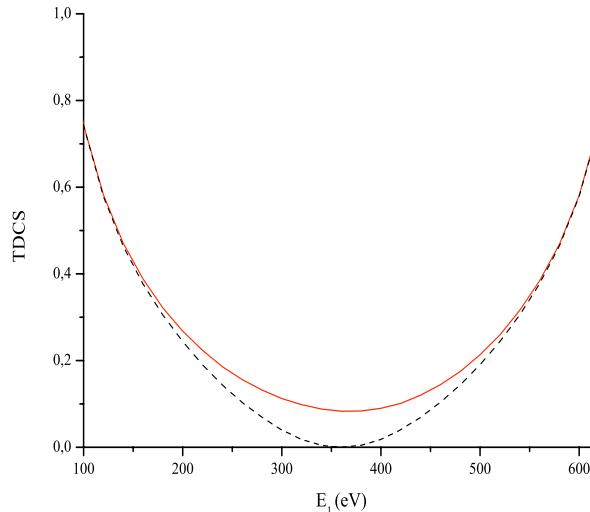


FIG. 6: (Color online) Electron energy distribution of the TDCS in $\text{mb eV}^{-1} \text{sr}^{-2}$. Electrons move in opposite directions with $\theta = 45^\circ$, $\varphi = 0$ and $\omega = 799 \text{ eV}$. Solid line, $k = \alpha\omega$, dashed line, $k = 0$.

type of structure whereas for zero photon momentum, it is uniformly zero. Note that for $\beta = 0$ (linear polarization), this distribution reduces to the one given in Fig. 2. It is interesting to analyze for what value of β , the effects due to nonzero photon momentum is the strongest. In Fig. 5, we show the TDCS for $\theta = 90^\circ$ and $\varphi = 135^\circ$ as a function of β for the same case as before, namely, $k = \alpha\omega$, a photon energy of 799 eV and $E_1 = E_2 = 360 \text{ eV}$. We clearly see that the TDCS reaches its highest value for $|\beta| \gtrsim 75^\circ$, *i.e.* for a highly elliptical polarization. It is interesting to note that if we were able to create a beam of such highly elliptically polarized photons, we would practically double the TDCS in comparison to the linear polarization. Note that for $\beta = 0$ (linear polarization), the TDCS is equal to zero. This results from the fact that $\theta = 90^\circ$ and $\varphi = 135^\circ$ (see Fig. 2).

Let us now study the electron energy distribution in the case the field polarization is linear. As before, we assume that both electrons are emitted back-to-back and consider the same case as in Fig. 2 namely a photon energy of 799 eV and a photon momentum given by $k = \alpha\omega$. We also set $\theta = 45^\circ$ and $\varphi = 0$. This corresponds to a maximum of the TDCS in Fig. 2. The results for the energy distribution are shown in Fig. 6 where they are compared with those obtained with $k = 0$. We clearly observe an effect resulting from the nonzero value of the photon momentum for $E_1 = E_2 = 360 \text{ eV}$. Note however that at $E_1 = E_2 = E$, the TDCS does not exhibit a local maximum. This is because, there is no integration on the solid angles Ω_1 and Ω_2 .

In Fig. 7, we study how the maximal value of the TDCS that occurs at $\theta = 45^\circ$ and $\varphi = 0$ (see Fig. 2) varies with the energy E of each electron or, in other words, with the photon energy. As before, it is assumed that both electrons are emitted back-to-back. Quite unexpectedly, we clearly see that the amplitude of the maximum of the TDCS occurs at the rather low energy $E \approx 10 \text{ eV}$ that corresponds to a photon energy of about 100 eV. In addition, the results presented in Fig. 7 demonstrate clearly that the amplitude of the effects due to the nonzero photon momentum depends strongly on the way the final state electron correlation is treated. In the case of the 3C function, the amplitude of the maximum of the TDCS near $E = 10 \text{ eV}$ is almost eight times the value obtained by using an uncorrelated 2C function to describe the final state wave function. Note that for values of $E > 80 \text{ eV}$, both functions lead to very similar results as expected. This dependence of the TDCS on the final state electron correlations confirms what was already suggested in Amusia's work [1].

Within the present context, it is legitimate to ask whether helium is the best target to observe effects due to nonzero photon momentum. In order to answer to that question, let us consider helium-like ions and examine the influence of the nucleus charge Z on the relative amplitude of the effects of nonzero photon momentum on the TDCS. We assume the external field linearly polarized and consider a back-to-back electron emission with $\theta = 45^\circ$, and $\varphi = 0^\circ$ since this configuration leads to a maximum of the TDCS for $k \neq 0$ as shown in Fig. 2. The ground states wave functions for a few light helium-like ions are generated following a procedure described in [9]. Our results are presented in Table 1. For each ion, we calculate the energy of the escaping electrons that lead to a maximum of the TDCS in the above configuration. We clearly see that for increasing values of the nucleus charge Z , the absolute value of the maximum of

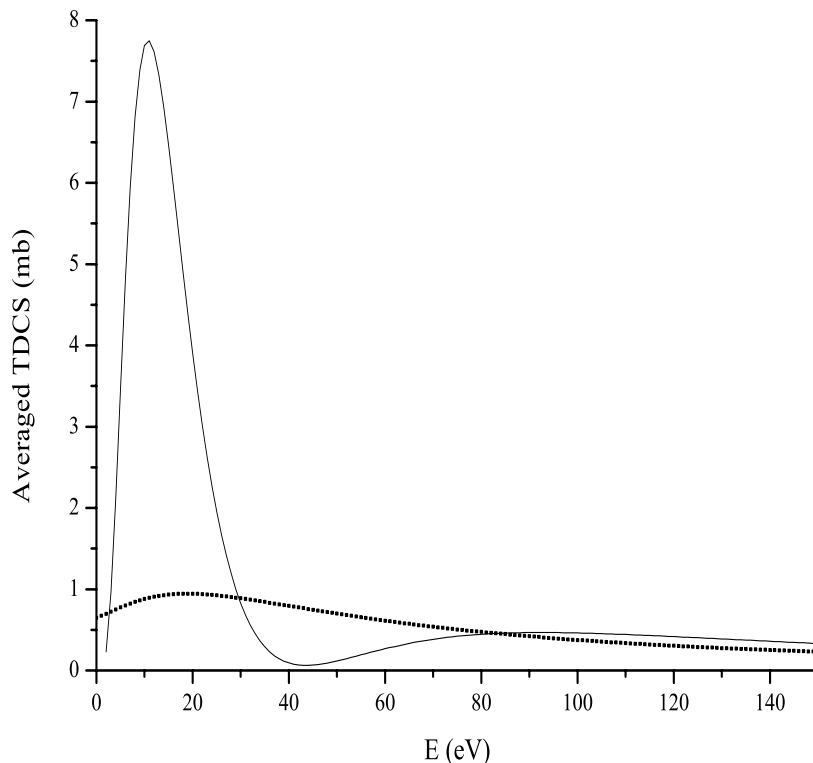


FIG. 7: Dependence of the maximum of the TDCS (in $\text{mb eV}^{-1} \text{sr}^{-2}$) on the energy $E = E_1 = E_2$ of the outgoing electrons moving in opposite directions with $\theta = 45^\circ$, $\varphi = 0$ and $k = \alpha\omega$. The solid line corresponds to a 3C final state wave function and the dotted line to the uncorrelated 2C final state wave function.

TABLE I: Energy $E = E_1 = E_2$ of the escaping electrons leading to a maximum value of the TDCS assuming a back-to-back electron emission with $\theta = 45^\circ$ and $\varphi = 0^\circ$. Various nucleus charges Z of helium-like ions are considered.

Z	E (eV)	maximum of TDCS (mb)
2	11	7,75
3	21	1,45
4	33	0,47
5	45	0,19
6	75	0,10

the TDCS decreases rapidly. Taking into account that the effects due to nonzero photon momentum are very small, it follows that from the experimental point of view, only helium and may be lithium are suitable targets.

IV. CONCLUSIONS

In this contribution, we considered $(\gamma, 2e)$ processes and studied in detail the effects resulting from nonzero value of the photon momentum on the triply-differential cross section. Due to the small value of the photon momentum, these

effects are quite small, of the order of a few mb, and are only observable in particular kinematical conditions. It is the case when both electrons are emitted back-to-back with equal energy sharing. In fact, for this configuration, the wave function has a node when the photon momentum is identically zero (dipole approximation). In these conditions, the absolute value of the effect depends on the energy and the polarization of the photon. The effect is the strongest when the polarization is linear or strongly elliptical. Furthermore and quite unexpectedly, we have shown that the effect is maximal for relatively low photon energies. We have also shown that the final state electron correlations play an important role. Neglecting electron correlations in the final state leads to a quite severe underestimation of the amplitude of the effect. Finally, we examined the case of several helium-like ions and showed that in the same kinematical conditions, helium or may be lithium are more suitable targets for observing experimentally these effects due to nonzero photon momentum.

Acknowledgements

We are grateful to Th. Weber for stimulating discussions. Yu.V.P. thanks the Université catholique de Louvain for hospitality and financial support. A.G., O.Ch. and Yu.V.P. acknowledge the Russian Foundation for Basic Research (grant no. 11-01-00523) for financial support. O. Ch. thanks a financial support from the theme 09-6-1060-2005/2013 “Mathematical support of experimental and theoretical studies conducted by JINR”. We also express our gratitude to Faculty of Computer Mathematics and Cybernetics of Moscow State University for providing access to the supercomputer Blue Gene/P.

-
- [1] M. Ya. Amusia, E. G. Drukarev, V. G. Gorshkov, and M. P. Kazachkov, *J. Phys. B: At. Mol. Phys.* **8**, 1248 (1975).
 - [2] J. A. Ludlow, J. Colgan, Teck-Ghee Lee, M. S. Pindzola, and F. Robicheaux, *J. Phys. B: At. Mol. Opt. Phys.* **42**, 225204 (2009).
 - [3] M. S. Schoffler *et al.*, *Abstracts of XXVII ICPEAC*, Th132 (2011).
 - [4] M. Ya. Amusia, *Atomic photoeffect* (NY: Plenum Press) (1990).
 - [5] J. S. Briggs and V. Schmidt, *J. Phys. B: At. Mol. Opt. Phys.* **33**, R1 (2000).
 - [6] O. Chuluunbaatar, H. Bachau, Yu. V. Popov, B. Piraux, and K. Stefanska, *Phys. Rev. A* **81**, 063424 (2010).
 - [7] O. Schwartzkopf and V. Schmidt, *J. Phys. B: At. Mol. Opt. Phys.* **28**, 2847 (1995).
 - [8] H. Brauning *et al.*, *J. Phys. B: At. Mol. Opt. Phys.* **31**, 5149 (1998).
 - [9] O. Chuluunbaatar, I. V. Puzinin, P. S. Vinitzky, Yu. V. Popov, K. A. Kouzakov, and C. Dal Cappello, *Phys. Rev. A* **74**, 014703 (2006).